

Modeling Hair Influenced by Water and Styling Products

Kelly Ward Nico Galoppo Ming C. Lin
University of North Carolina at Chapel Hill
{wardk,nico,lin}@cs.unc.edu

Abstract

We present novel methods for capturing the key characteristics of hair influenced by water and styling products. Our approach includes a dynamics system that adaptively accounts for changing stiffness and weight of the hair, a geometric representation that can alter the physical depiction of hair based on the substance(s) present on it, and a rendering approach to account for the varying appearance of hair. Additionally, strands of hair can dynamically bond together due to the introduction of water or styling products. All of these properties can vary on the fly as water or styling products are applied to the hair.

1 Introduction

Realistically simulating the motion and appearance of hair is an important goal in modeling virtual humans for many applications. In the real world, external substances interact with hair, thereby changing its physical behavior and outward appearance. Existing hair modeling systems, however, have primarily focused on depicting the basic properties of hair, free of any external influences. By capturing the essential attributes of hair influenced by water and styling products, an enhanced hair modeling system can be used by beauticians, stylists, dermatologists and other physicians to “preview” the hair appearance and movement under different conditions.

Main Results: In this paper, we introduce several fundamental techniques for modeling hair

that capture the key features of hair appearance and behavior affected by external substances. The main results are:

- A dual-skeleton system that decouples the control of the local and global behavior of hair providing an efficient localized collision detection method;
- Automatic adjustment of dynamic properties of hair due to external substances;
- Design of flexible geometric structures that account for frequently changing hair volume;
- “Dynamic bonds” that model the adhesive forces introduced by styling chemicals to the hair;
- Approximation of lighting equations by parameterizing the key factors that affect the visual appearance of wet hair.

Organization: Related work on hair modeling is briefly reviewed in Section 2. Section 3 presents some basic properties of hair in the presence of water and styling products. The key elements of our improved hair modeling system are described in Section 4. The methods for achieving the desired characteristics of hair behavior and appearance due to the presence of water and styling products are explained in Sections 5 and 6, respectively. Discussion of our implementation and demonstration of the results thereof are provided in Section 7. Finally, we conclude with some future research directions.

2 Previous Work

2.1 Hair Modeling

Many techniques have been proposed to model hair dynamics. Individual strands can be represented as a series of open chains of line segments and hairstyles are specified by using the angles between them [1, 2, 3]. Groups of hair strands that are in close proximity of one another can be grouped together as “wisps”, each with a single skeleton to control motion [3, 4, 5, 6]. Similarly, guide strands can be used to interpolate the motion of the guide skeleton to the nearby strands within each hair cluster [7]. Fluid dynamics have been used in combination with individual strand dynamics to capture the complex interactions of hair [8]. The work of [9] produced hair-gel effects by retaining a deformed hairstyle shape where the product was applied.

Most recently, multiresolution representations, either using a hierarchy of hair clusters for styling [10], a combination of three discrete representations (strands, clusters, and strips) [11], or continuous, adaptive subdivision [12, 13], have also been proposed to further speed up the performance for hairstyling, modeling and simulation.

2.2 Hair Rendering

An anisotropic lighting model for hair was presented in [14], which was efficiently implemented with texture maps by [15]. Self-shadowing due to intra-hair occlusion is a vital feature. Opacity shadow maps [16] are less expensive than deep shadow maps [17] providing similar visual effects. Most recently, [18] introduced a new shading model that accounts for various light scattering effects, generating photorealistic appearances of hair.

3 Background

Before we describe our method for capturing the primary effects of water and styling products on hair, it is important to understand some physical properties of hair fibers and their interaction with these substances.

3.1 Hair and Water

Hairs of most mammals, including humans, mainly consist of the protein material α -keratin [19]. Water acts as a plasticizer of the biopolymeric structure of keratin and is able to drastically modify many of the physical properties of α -keratin fibers, including mechanical and electrical properties. As a plasticizer, water changes the longitudinal stiffness of fibers by as much as a factor of three as water is fully absorbed into the hair. Furthermore, hair fibers are highly permeable allowing hair to absorb 30 to 45% of its own weight in water causing the fibers to swell radially by about 16% as the hairs’ wetness increases [20, 19].

While individual hair fibers swell due to the absorption of water, wet strands in close proximity with each other group together due to the bonding nature of water. As a result, wet hair appears less voluminous in comparison to dry hair. Figure 1 shows side by side images of a real person with wet and dry hair. Note how much fuller the hair is when it is dry than when it is wet.

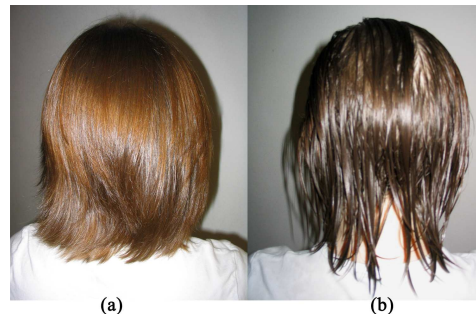


Figure 1: Real images of (a) dry and (b) wet hair.

3.2 Hair and Styling Products

The purpose of cosmetic styling, or fixative, products is to change the physical properties of hair. Given the myriad of fixative products on the market, we have chosen to look at the general effects of styling aids on hair. The functions of styling products are typically to hold a section of hair in place, alter the feel of hair, and/or increase the inter-fibril interactions of hair strands [19]. The application of fixative products prevents fibers from smoothly sliding over each other.

Fixative products usually cause a high degree of adhesiveness in hair, thereby causing

hair strands to cling together and move in large groups wherever the product is applied. Polymers constitute the primary active ingredient of most styling products and they increase the stiffness of the hair fibers, thus decreasing the general motion of the hair. The most observable effects of fixative products are typically stiff hair motion and the bundling of strands [19]. Figure 2 shows hair with and without styling products.



Figure 2: Real images of hair (a) without and (b) with styling products (hairspray).

4 Hair System

Here we introduce some of the key concepts for our hair modeling system.

4.1 Motivation for Dual-skeleton System

Hair motion is subject to changes in the global positioning of the strands, as well as localized styling changes such as the elongation of a curl under force. While the localized styling motion can be made very stiff through the application of a strong fixative product, the hair is still subject to a global motion when forces are applied to it.

Wisp-based hair modeling systems, such as [5, 12], have solved this problem by using a single skeleton curve modeled as a set of particles connected with rigid springs and hinges. Wavy hairs are produced by specifying the number of waves and amplitude of waves inside each wisp. As the wisp segment stretches, the amplitude and frequency of the waves are adjusted to show the wavy hair stretching straight.

The single skeleton dynamics can capture the deforming hairstyle, however there are no checks to ensure that the length of the hair is preserved over time or that the collision detection

remains both accurate and efficient throughout the simulation in light of the changing orientation and position of the hair inside of the wisp.

In order to capture both the global motion and localized styling motion of hair, to ensure hair length preservation at all time, and to maintain an accurate and efficient collision detection method throughout the simulation, we have created a *dual-skeleton* system for modeling hair. This dual-skeleton system provides a single skeleton to control the global motion of hair and a second one to provide a positioning guide and localized collision detection scheme for hair. We refer to these skeletons as the *global-skeleton* and the *local-skeleton*, respectively.

4.2 Dual-skeleton Setup

The global-skeleton is modeled as a series of line segments connected by node points, $N_{g0}, N_{g1}, \dots, N_{g(n-1)}$, where n is the number of node points. A hairstyle is defined by positioning the local-skeleton in the desired form in relation to the global-skeleton, see Figure 3. Let the line segment between the N_{gi} and $N_{g(i-1)}$ global-skeleton node points be the i th global-skeleton segment, S_{gi} . The i th local-skeleton node, N_{li} , lies in the plane perpendicular to S_{gi} containing N_{gi} . Each local-skeleton node has a defined angular position to fix it around the global-skeleton segment.

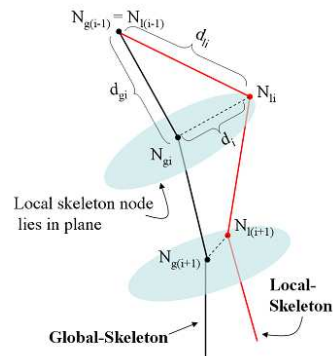


Figure 3: Positioning of the local-skeleton relative to the global-skeleton.

The rendered hair geometry follows the form of the local-skeleton. The hair strands are modeled as subdivision curves [11]. Strands in close proximity with each other are grouped together to follow the same dual-skeleton system. This grouping helps to capture the natural

clumping of strands due to external substances or electrostatic forces that can be found in nature. Once the dual-skeletons are created, circular cross-sections are defined at each node point of the local-skeleton. The strands of hair are placed randomly within the bounds of the cross-sections.

4.3 Dynamics Model

There are two types of motion controlling the global-skeleton. The first dictates the bending of the strands by maintaining a spring force to control the angular position of each node point in relation to its neighbors. Second, soft springs are used to control the elongation of the global-skeleton. Each global-skeleton section is prevented from stretching beyond the reach of its corresponding local-skeleton section since the length of the local-skeleton is preserved at all times. For straight hair the nodes of the global-skeleton are connected with rigid links and the position of the local-skeleton is equal to that of the global skeleton.

The only value to compute for updating the position of the local-skeleton node is the distance of the node point from its corresponding global-skeleton node point (see Figure 3). First, the current distance between N_{gi} and $N_{g(i-1)}$ is calculated, d_{gi} . The root node, N_{g0} , of the local-skeleton is set equal to the root node of the global-skeleton. The distance between N_{li} and $N_{l(i-1)}$ of the local-skeleton is fixed, d_{li} . Therefore, d_i , the distance of N_{li} from N_{gi} , is calculated by:

$$d_i = \sqrt{d_{li}^2 - d_{gi}^2}$$

Thus, as the global-skeleton elongates, increasing d_{gi} , the local-skeleton straightens and the node points of the local-skeleton move closer to the global-skeleton, decreasing d_i .

4.4 Localized Collision Detection

The local-skeleton is used for collision detection since the rendered strands adhere to its motion. We utilize the collision detection system proposed by [11, 13], which uses *swept sphere volumes* (SSVs) [21] to encapsulate the hair. The radii of the cross-sections at each local-skeleton node point define the offset for the SSVs.

When a collision is detected between the hair and body, the global-skeleton of the hair section is moved so that the local-skeleton (and hair geometry) are outside of the body. All positional changes are first made on the global-skeleton and the local-skeleton follows the changes as described in Section 4.2. It is important to note that if the global-skeleton collides with an object, but the SSVs of the hair, and the corresponding local-skeleton, do not collide with the object, then no action is taken.

Moreover, our method efficiently detects hair-hair collisions by decomposing the space encompassing the hair into three-dimensional grids. SSVs that fall in the same grid cell are tested against each other for overlap. If two sections of hair overlap, we use the response method of [5, 13] to push apart the hair sections based on their respective orientations.

This localized collision detection method allows the local-skeleton to be positioned farther away from the global-skeleton, increasing d_i , while maintaining accurate collision detection. This approach results in creating full, voluminous hair. Our dual-skeleton system is thus able to model more diverse types of hairstyles than most existing techniques.

5 Modifications of Physical Properties

We now account for various physical changes that occur when hair absorbs water or when fixative products are applied. The main characteristics we emphasize are:

- **Adjusting dynamics properties** to account for changing mass and spring stiffness of the hairs *on-the-fly*;
- **Flexible geometric structure** to allow the hair volume to change due to the presence of external substances;
- **Bonds between strands** that form and break *dynamically* reflecting the connection of strands due to water or styling products.

5.1 Adjustment of Dynamic Properties

The first two physical changes on hair we account for are the changes in mass and spring stiffness. As water is absorbed into hair fibers,

the mass of the hair increases up to 45% and the stiffness of the hair fibers increases by a factor of three. As styling products are applied to hair, the stiffness of the hair is increased and the mass of the hair is also increased due to the presence of additional substances.

External forces, such as wind and gravity, are applied to the node points following the standard equation of force:

$$F_i = m_i * a_i$$

F_i is the force applied to the i th node, m_i and a_i are the mass and acceleration of the i th node, respectively. We vary the mass of the nodes to correspond to the length of the strand representing the nonuniform weight of strands from the root of the strand to its tip.

As the fraction of wetness of the hair, $f_{wetness}$, increases to 100%, the mass of the hair increases up to 45% of its initial dry weight. The mass of the i th node, m_i , is then calculated as:

$$m_i = m_{dry_i} + (m_{dry_i} * 45\%)f_{wetness}$$

where m_{dry_i} is the initial, dry mass of the i th node.

The internal forces acting on each node point i consist of angular torque, M_{θ_i} and M_{ϕ_i} for the θ and ϕ components, as well as the spring force controlling the length of each global-skeleton section, F_{len_i} . All of these internal forces are spring forces containing separate spring constants, k_{θ_i} , k_{ϕ_i} , k_{len_i} , respectively. The final spring force equations become:

$$\begin{aligned} M_{\theta_i} &= -k_{\theta_i}(\theta_i - \theta_{i0}), \\ M_{\phi_i} &= -k_{\phi_i}(\phi_i - \phi_{i0}), \\ F_{len_i} &= -k_{len_i}(d_{gi} - d_{gi0}), \end{aligned}$$

where θ_i , ϕ_i , θ_{i0} , ϕ_{i0} are the current angle values and resting angles of the i th node in polar coordinates, respectively and d_{gi} and d_{gi0} are the current and resting lengths of the i th segment of the global-skeleton, respectively. With a high, or stiff, k_{len} value, the hair will be able to bend freely in the θ and ϕ directions, but will not stretch or compress as liberally.

As styling products are applied to the hair, the spring constant k_{len} is increased. We found that by increasing just the k_{len} value we obtained motion results similar to that of hairspray and other fixative products. The amount to increase the stiffness depends on the product that is being used. However, we found that by using an implicit integration technique [13], we were able to increase this spring constant by a factor of 10 and maintain a stable simulation.

5.2 Flexible Geometric Structure

As explained in Section 3.1, as hair gets wet it becomes less voluminous. To account for this property, when water is applied to the hair, the radii of the hair sections decrease accordingly. At 100% wetness, the thickness of a group of strands will be equal to the number of strands times the thickness of a strand:

$$\begin{aligned} AreaOfGroup &= (AreaOfStrand) * n; \\ WR_i &= \sqrt{n} * r \end{aligned}$$

where WR_i is the radius of the i th cross-section at 100% wetness, n is the number of strands in the current strand group, and r is the radius of a single strand.

We extend this radius contraction to variable amounts of wetness by creating a linear relationship based on the amount of wetness in the system:

$$CR_i = DR_i - (DR_i - WR_i)f_{wetness}$$

where CR_i is the current radius of the i th cross-section, DR_i is the dry radius of the i th cross-section, and $f_{wetness}$ is the fraction of water absorbed at the given time.

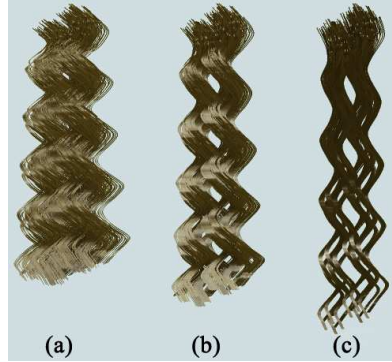


Figure 4: Sections of curly hair progressively getting wet: (a) 0% wetness (dry) (b) 50% wetness (c) 100% wetness.

Not all strands of hair are exactly the same length, so our system reflects this observation by varying the radius at each level of the strand grouping. These effects are illustrated in Figure 4, which shows a section of curly hair at 0%, 50%, and 100% wetness.

As the radii of the strand groups fluctuate, the offsets of the SSVs used for collision detection are automatically updated reflecting the change. This process is performed on-the-fly allowing the radii of the strand groups to change dynamically.

5.3 Dynamic Bonds between Strands

Due to the bonding effects of most fixative products, hair strands tend to adhere to each other where the product has been applied. We have extended the use of the *static links* exercised in [7], which were used as breakable connections between guide strands to enable hairstyle recovery. In [7], these links were selected and setup at the beginning of a hair simulation and were broken when they encountered excessive forces. In our system, “dynamic bonds” that model bonding forces between sections of hair are created on-the-fly when fixative products are applied. They can be created at any point in a simulation at any place along the dual-skeletons.

Our dynamic bonds are modeled as spring forces connecting two separate nodes of nearby global-skeletons. Our hair-hair collision detection method, described in Section 4.4, identifies which sections of hair are touching. When a styling product is applied to the hair, each section of hair maintains a list of the hair sections with which it is in contact. The dynamic bonds are then formed connecting the corresponding sections. A single section can have as many bonds as hair sections it is touching. The new bonding spring force, f_{bond} , between two global-skeleton nodes becomes:

$$f_{bond} = -k_{bond}(d_{current} - d_{initial})$$

where k_{bond} is the spring constant of the bond, $d_{current}$ is the current distance between the nodes and $d_{initial}$ is the distance between the two nodes when the fixative product is first applied.

Following methods similar to [7], these bonds are broken when a large force is applied to it. The force required to break the bond is directly related to the strength of the spring constant k_{bond} , which is determined based on the amount and strength of fixative product applied.

These dynamically forming and breaking bonds cause large sections of hair to group together and move in union, reflecting the clumping effect of real fixative products. Moreover, these bonds restrict the strands’ ability to move over or past each other, an effect exhibited in real hairs due to the increased frictional force caused by fixative products on hair [19].

6 Rendering

We model the hair strand reflections by light scattered from a cylindrical surface[14] and encode an anisotropic lighting equation in a texture map as in [15]. Self-shadows are generated by accumulating the opacity α of the strands hit by the light rays along the light direction in the hardware framebuffer, a technique called *opacity shadow maps* [16].

6.1 Influence of Wetness

Wetness can make objects look darker, brighter, and/or more specular. As noted by [22], the differences in appearance are caused by a combination of the presence of liquid on the surface and inside the material. When hair becomes wet, a thin film of water is formed around the fibers. The rough, tiled air-fiber interface, observed by [18], changes to a smooth, mirror-like air-water interface. Obviously, this change gives the hair a shinier appearance due to specular reflections, typically modeled by an increasing fall-off exponent in the Phong illumination shading model.

Due to water absorbed inside and surrounding the hair fibers, the relative index of refraction decreases. The absorption of light inside the hair then increases due to a greater amount of total internal reflection. This phenomenon causes a darker appearance of wet hair in comparison to dry hair. The increased opacity value also leads to more aggressive self-shadowing.

Moreover, this relation implies that a smaller fraction of light that is radiated by the hair has traversed the fiber core. Hair fibers have a pigmented core at the center of the cylindrical volume, the source of its apparent color. Therefore, only the fraction of light rays that traversed the hair core are responsible for the color we observe [18]. Consequently, with increasing wetness, the hair radiates an increasing fraction of colorless light, originated at the air-water surface reflections. This effect contributes to the shinier appearance of wet hair over dry.

The three main parameters in our shading algorithm are: α , which controls the opacity shadow map [16], s is the exponent for the specular reflection term, and f_a determines the contribution of (partly) non-colored anisotropic reflection. The rendering equation for each hair

strand can be expressed as:

$$I_o = (1 - f_a)k_a I_d + f_a(k_d \langle L, N' \rangle + k_s \langle V, R \rangle^s) I_i$$

where L is the light direction, N' is the projection of the light vector L onto the normal plane [15], and R is the reflected direction. The diffuse color $k_a I_d$ is simply the strand color, while the incoming light from the scene is I_i .

We have captured the interactions of light with the wet strands by varying the rendering parameters based on the amount of water present on the hair. More specifically, we control the parameter vector $\mathbf{V}_p = [\alpha, s, f_a]$. Extreme values are empirically obtained, defined by \mathbf{V}_p^{min} and \mathbf{V}_p^{max} . Depending on the wetness percentage $f_{wetness}$, we then linearly interpolate according to the following formula:

$$\mathbf{V}_p = \mathbf{V}_p^{min} + f_{wetness}(\mathbf{V}_p^{max} - \mathbf{V}_p^{min})$$

As the wetness factor varies between 0% and 100%, the parameters vary accordingly, creating a damped or wet look for the hair strands.

7 Results and Analysis

We have implemented our hair modeling system in C++ and displayed the images using OpenGL.

7.1 Comparison

The results of our simulations are illustrated in Figure 5, showing, from left to right, the same hairstyle (red long, curly hair) blowing in the wind with different effects. Note that the wet hair is not as voluminous as the dry hair. Also, the hair with fixative products present retains tighter curls than the dry hair when carried by the wind, and moves together in larger bundles of hair. For further demonstrations and additional images, please visit our project website:

<http://gamma.cs.unc.edu/HairWS>

Our system requires no pre-computations to dynamically add water or styling products to the hair. As a result, our simulations run at approximately the same rate with or without external substances present. On average the results took 4.16 seconds per frame for simulation and 0.34 seconds per frame for rendering. Timings were taken on a PC with a 1.8 Ghz processor, 1 GB RAM, and a GeForce 4 graphics card, for the hair shown in Figure 5. This hairstyle has an average of 16 nodes per strand and a total of 9,680 rendered strands.

7.2 Limitations

Our current implementation applies a general wetness factor, as well as amount and type of fixative product, to the entire head of hair to illustrate the general effects of the substances on the hair. However, the ability to apply water and styling products to a specific section of hair is a feature that would be useful to an interactive virtual hairstyling system.

Furthermore, while a ray-tracing or photon-mapping implementation would give more accurate rendering results, we chose to use an approximate, faster rendering algorithm so that our work could be easily integrated with techniques using multiresolution representations [10, 11, 12, 13] for interactive styling.

8 Conclusion and Future Work

We presented several simple yet effective techniques to account for the influence of water and styling products on hair behavior and visual appearance. The methods we have presented may be used together or integrated separately into varying hair modeling schemes. We plan to integrate these techniques with multiresolution representations [10, 11, 12, 13] to further improve runtime performance and integrate the resulting system with a 3D interface for interactive virtual hairstyling.

Acknowledgements

This project is supported in part by Intel Corporation, Army Research Office, National Science Foundation and Office of Naval Research.

References

- [1] K. Anjyo, Y. Usami, and T. Kurihara. A simple method for extracting the natural beauty of hair. *Computer Graphics*, 26(2):111–120, 1992.
- [2] A. Daldegan, T. Kurihara, N. Magnenat-Thalmann, and D. Thalmann. An integrated system for modeling, animating and rendering hair. *Computer Graphics Forum (Proc. of Eurographics)*, 12(3):211–221, 1993.
- [3] T. Kurihara, K. Anjyo, and D. Thalmann. Hair animation with collision detection, models and



Figure 5: Comparison images of long, curly, red hair blowing in the wind. From left to right: showing (1) hair at 100% wetness (2) clean, dry hair (3) hair with fixative products present.

- techniques. *Proc. of Computer Animation*, pages 128–138, 1993.
- [4] L. H. Chen, S. Saeyor, H. Dohi, and M. Ishizuka. A system of 3d hair style synthesis based on the wisp model. *Visual Computer*, 15(4):159–170, 1999.
- [5] E. Plante, M. Cani, and P. Poulin. Capturing the complexity of hair motion. *GMOD*, 64(1), Jan 2002.
- [6] Z. Xu and X. D. Yang. V-hairstudio: An interactive tool for hair design. *IEEE Computer Graphics and Applications*, 21(3):36–43, 2001.
- [7] J. Chang, J. Jin, and Y. Yu. A practical model for hair mutual interactions. *Proc. of ACM Symposium on Computer Animation*, 2002.
- [8] S. Hadap and N. Magnenat-Thalmann. Modeling dynamic hair as a continuum. *Computer Graphics Forum (Proc. of Eurographics 2001)*, 20(3), 2001.
- [9] D.-W. Lee and H.-S. Ko. Natural hairstyle modeling and animation. *Graphical Models*, 63(2):67–85, March 2001.
- [10] T.-Y. Kim and U. Neumann. Interactive multiresolution hair modeling and editing. *Proc. of SIGGRAPH*, 2002.
- [11] K. Ward, M. Lin, J. Lee, S. Fisher, and D. Macri. Modeling hair using level of detail representations. *Proc. of Computer Animation and Social Agents*, 2003.
- [12] F. Bertails, T.-Y. Kim, M.-P. Cani, and U. Neumann. Adaptive wisp tree - a multiresolution control structure for simulating dynamic clustering in hair motion. *Proc. of ACM SIGGRAPH / Eurographics Symposium on Computer Animation*, 2003.
- [13] K. Ward and M. Lin. Adaptive grouping and subdivision for simulating hair dynamics. *Proc. of Pacific Graphics*, 2003.
- [14] J. T. Kajiya and T. L. Kay. Rendering fur with three dimensional textures. In Jeffrey Lane, editor, *Computer Graphics (SIGGRAPH '89 Proceedings)*, volume 23, pages 271–280, July 1989.
- [15] W. Heidrich and H.-P. Seidel. Efficient rendering of anisotropic surfaces using computer graphics hardware. *Proc. of Image and Multi-dimensional Digital Signal Processing Workshop (IMDSP)*, 1998.
- [16] T.-Y. Kim and U. Neumann. Opacity shadow maps. *Proc. of Eurographics Rendering Workshop*, 2001.
- [17] T. Lokovic and E. Veach. Deep shadow maps. In *Proceedings of ACM SIGGRAPH 2000*, pages 385–392, 2000.
- [18] S. R. Marschner, H. W. Jensen, M. Cammarano, S. Worley, and P. Hanrahan. Light scattering from human hair fibers. *ACM Trans. Graph.*, 22(3):780–791, 2003.
- [19] D. Johnson. *Hair and Hair Care; Cosmetic Science and Technology Series*, volume 17. New York Marcel Dekker, Inc., 1997.
- [20] L’Oreal. <http://www.loreal.com>, 2004.
- [21] E. Larsen, S. Gottschalk, M. Lin, and D. Manocha. Distance queries with rectangular swept sphere volumes. *Proc. of IEEE Int. Conference on Robotics and Automation*, 2000.
- [22] H. W. Jensen, J. Legakis, and J. Dorsey. Rendering of wet material. *Rendering Techniques*, pages 273–282, 1999.